*Bulletin of the New Zealand Society for Earthquake Engineering, Vol. 58, No. 4, December 2025*

# GROUND MOTION SIMULATIONS FOR DUNEDIN AND MOSGIEL, OTAGO, NEW ZEALAND

**Anna Kowal[1], Mark Stirling[1] and Seokho Jeong[2]**

(Submitted *November 2024*; Reviewed *January 2025*; Accepted *March 2025*)

**ABSTRACT**

We develop large scenario earthquakes on active faults in the vicinity of Dunedin and use them to develop ground motion simulations for a site in Dunedin (St Kilda – St Clair area, referred to as "St Beach") and Mosgiel (centre of Mosgiel, referred to as "Taieri Basin"). The scenarios are developed to represent large Akatore Fault (within 15 km of Dunedin and Mosgiel) and Hyde Fault (within 40-50 km) earthquakes. The simulations utilise the Southern California Earthquake Centre Broadband Simulation Platform and the Graves–Pitarka simulation method. Site response analysis is conducted with two-dimensional basin models, and the nonlinear finite element software OpenSees. The dynamic response characteristics of the soft sedimentary layers are modelled with a pressure-independent multi-yield plasticity model. Some confidence in the simulation method is gained by undertaking historical validations, using the only instrumentally recorded earthquake of significance in the region (the $M_w$ 4.7 2015 Lees Valley earthquake). The simulations provide close matches to the amplitudes and durations of the recorded time histories. The Akatore and Hyde fault earthquake simulations show peak ground accelerations of up to 0.8 g and 0.3g respectively, with durations of strong shaking of around 10 to 20 seconds. Uncertainty in the simulated ground motions due to source is quantified by comparing the spectra for repeated simulations, in which the range of source parameters are sampled. The resulting range of simulations shows a spread of as much as 0.5g. The Akatore – St Beach spectra are also compared to NZS1170.5 and New Zealand national seismic hazard model 2022 (NZ NSHM 2022) spectra, for site classes relevant to those of the St Beach site. In general, the simulated spectra exceed the NZS1170.5 spectra at the 0.1-0.3 second periods, but are similar to the mean NZ NSHM 2022 spectra at these periods. Future updates to NZS1170.5 based on NZ NSHM 2022 will therefore be expected to produce design spectra that are more consistent with the results of our study. The study represents the first ground motion simulations developed for southern New Zealand, and the simulation methods could be used to further advance understanding of seismic hazard in the region.

https://doi.org/10.5459/bnzsee.1725

## INTRODUCTION

Earthquake hazards present a significant risk to life and property in New Zealand. Many active faults are located near densely populated areas, and industrial/infrastructural developments. A simplistic way of communicating hazard information is through earthquake scenarios. Scenarios provide key information on potential future earthquakes, such as magnitude, distance, and potential ground motions. A limitation of scenarios is that they do not provide a probabilistic context unless explicitly defined from disaggregation of probabilistic seismic hazard models [1]. Despite this limitation, earthquake scenarios developed for Christchurch [2] showed significant similarities to the mainshock and damaging aftershocks that occurred during the 2010–11 Canterbury earthquake sequence.

Scenario earthquake effects can be produced in a number of ways. Earthquake scenarios can be in the form of written descriptions, often relying on the Modified Mercalli Intensity scale. Another method is to use ground motion models to provide scenario response spectral accelerations, velocities and displacements based on the magnitude, distance, slip type, and ground conditions of the site. Finally, with the advent of significant computing power, physics-based ground motion simulations can be developed that compute synthetic time histories and response spectra as a function of the earthquake source [3], the path from the source to the site of interest [4], and the geological and geophysical conditions of the site [5] (see Figure 1). These can be simple 1D simulations, through to 3D simulations that include information on basin geometry.

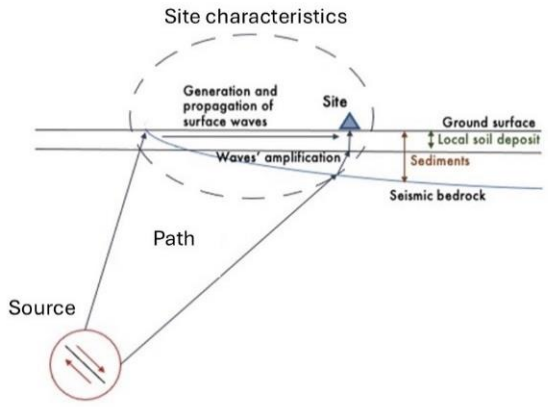


***Figure 1: The three critical factors that are considered in ground motion simulations: the source, the path, and the site characteristics.***

Physics-based simulations have been developed for many earthquake scenarios around New Zealand. Notable examples are Alpine Fault [6] and Hikurangi subduction zone scenario earthquakes (e.g. [7]). Simulations have been carried out for notable recent earthquakes, such as the $M_w$ 7.1 2010 Darfield,

[1] *Otago Earthquake Science Group, University of Otago, Dunedin, mark.stirling@otago.ac.nz (Fellow)*
[2] *Changwon National University, Changwon 51140, South Korea (non-member)*

and $M_w$ 7.8 2016 Kaikoura earthquakes (e.g. [8]). The advantage of developing simulations for well-recorded earthquakes is that the strong motion records can be used to test the performance of the simulation methods.

The centres of Dunedin and Mosgiel have not experienced any large earthquakes since first settled in approximately 1840. The most significant event in the area's history was a $M_w$ 4.7 event that occurred offshore to the south of the city in 1974. This magnitude is considerably smaller than the maximum-sized events ($M_w > 7$) that could occur on local active faults (e.g. [9]). The absence of experience in the Dunedin–Mosgiel area therefore makes the development of realistic earthquake scenarios important for engineering, public awareness, planning and preparedness.

Ground-motion simulation modelling has not been attempted in Dunedin and Mosgiel prior to this study [10], with seismic hazard studies limited to regional- and national-scale seismic hazard assessments [11-17].

In this study, we develop large scenario earthquakes for two local sources (Akatore and Hyde faults) as shown in Figure 2, and then use these scenarios and open-source software (the Southern California Broadband Simulation Platform, or SCEC BBP; [18]) to model ground motion simulations for two sites (south Dunedin and Mosgiel). Two-dimensional basin models and site response modelling methods are also applied, including use of the nonlinear finite element software OpenSees (opensees.berkeley.edu).

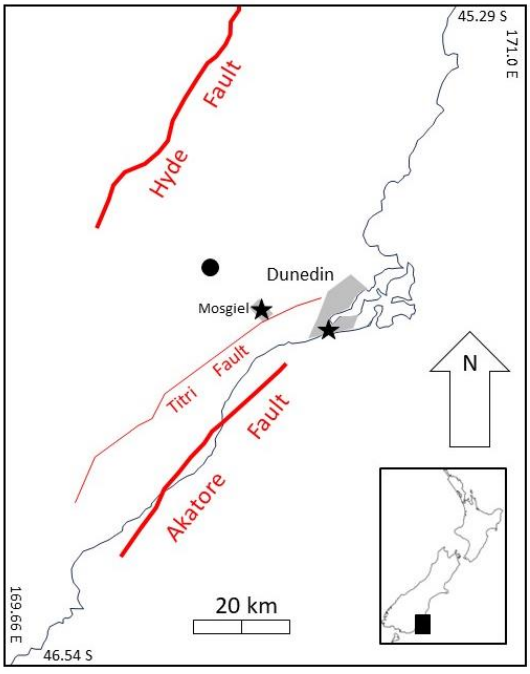


***Figure 2: The Akatore and Hyde fault sources, in relation to Dunedin and Mosgiel. The locations of the two sites are shown as stars, as well as the epicentre of the $M_w$ 4.7 2025 Lees Valley earthquake (black dot). The Titri Fault is also shown.***

Our ground-motion simulations are developed for earthquakes that have never been experienced before in Dunedin and Mosgiel. Therefore, it is important to use whatever methods are available to gain confidence in the simulations. This is achieved by using the same simulation methods to simulate well-recorded earthquakes, and then compare the simulations to the records. This is referred to as the historical validation approach [19].

Validations are performed using the only accelerogram-recorded local event of significance in the Dunedin–Mosgiel area. This was the $M_w$ 4.7, 1 June 2015 Lees Valley earthquake (geonet.org.nz; event ID 2015p4093980), which occurred approximately 30 km northwest of Dunedin (see Figure 2). This validation requires generating simulations at accelerograph sites for earthquakes of the same magnitude and source-to-site distance as the Lees Valley earthquake, and then comparing the results to the instrumental records.

## STUDY AREAS

### Sources

Dunedin and Mosgiel are located near the eastern edge of the transpressional boundary of the Pacific and Australian plates and are at the eastern edge of the Otago Range and Basin province (e.g. [9]). A series of northeast-striking reverse faults cross the region, and at least some of these faults are reactivated Cretaceous normal faults [20]. The two closest active faults to Dunedin and Mosgiel are the Akatore and Titri faults (see Figure 2). The Akatore Fault exhibits the most recent activity of the two, producing no less than three ground-rupturing earthquakes in the last 15,000 years, with two of them occurring in the last 1,000 years [9]. The Akatore Fault is also the only fault in the region that shows microseismicity at present [21], so may still be in a heightened state of activity following the earlier, major earthquakes. It is located about 15 km from Dunedin and Mosgiel. The Titri Fault is also located close to Dunedin and Mosgiel, but has exhibited much less frequent earthquake activity in the late Quaternary, with approximately 20,000 years having elapsed since the last event [22]. The third-closest known active fault to Dunedin and Mosgiel is the Hyde Fault. It is approximately 50 km from Dunedin and 40 km from Mosgiel (Figure 2), and it has also been a focus of recent paleoseismic investigations [23].

The Akatore and Hyde faults are selected for this study (Figure 2). The Titri Fault is not selected because the simulations for the Akatore and Titri faults would be similar for South Dunedin and Mosgiel due to their close source-to-site distances. Furthermore, the greater activity of the Akatore Fault makes it the more logical focus for the simulations. The Hyde Fault provides a scenario for an earthquake about 50 km from South Dunedin and 40 km from Mosgiel, so is representative of the many faults located to the west within central Otago (e.g. [23]).

### Site Selection

The two sites chosen for ground motion simulations are centred on South Dunedin and Mosgiel. As shown in Figures 2 and 3, the sites are chosen in the area of St Clair and St Kilda suburbs (hereafter referred to as "St Beach profile") and within Mosgiel (hereafter referred to as "Taieri Basin profile"). The sites are chosen on the basis of there being an availability of subsurface geological information, as well as being focused on two populated areas for maximum relevance.

The St Beach site is located within a tombolo that connects the Otago Peninsula to the mainland (Figure 3). The near-surface geology is dominated by dune-sand and swamp sediments, with well-sorted gravels containing sandy and silty pockets at greater depths [22,24-27]. These soft near-surface sediments form an approximately 25 m thick package which rests on the more competent rocks of the Dunedin Volcanic sequence and Cretaceous–Early-Mid Cenozoic sedimentary sequence.

The Taieri Basin site is located within a tectonic depression situated 6 km southwest of Dunedin city (Figure 3). The basin area is approximately 25 km long and 8 km wide, and the ground surface is very close to sea level [22]. The basement rock type is Otago Schist, and the basin is filled by a sequence of Cretaceous to late Quaternary sediments[28-30].

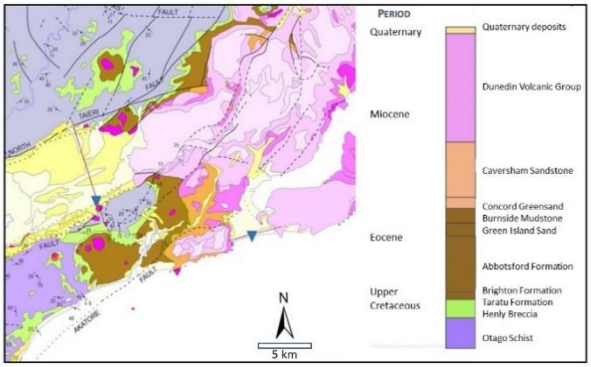


***Figure 3: Geological map of the study area, showing sites (inverted triangles) and associated profile lines (thin lines intersecting the inverted triangles) addressed in the study. The St Beach site/line is to the east, and the Taieri Basin site/line is to the west. Local geology is sourced from* [30], [31] and [32].**

### St Beach Profile Model

A profile line is defined at the St Beach site for development of a 2D basin model, and is shown in Figure 3. The St Beach profile is modelled as layers of sediments (soils), soft rock, and rock, and uses a plane strain formulation for the quadratic elements (see Figures 4 and 5). Specifically, analyses using a 2D cross section model will typically assume the plane strain condition, meaning the assumption of zero strain in the perpendicular direction. The column is defined down to 200 m depth based on site investigations, and general geological and geophysical knowledge of the area [33] The soil column shows 25 m of soft soil sandy sediments underlain by soft rock layers and hard Caversham sandstone (Figure 5). The shear wave velocity $V_s$ and mass density $\rho$ values are also shown in Figure 5, and the model parameters are shown in Table 1.

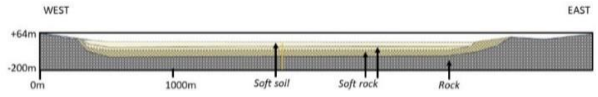


***Figure 4: The St Beach profile model. The "Soft soil" layers represent layers 4 to 6 from Table 1, "Soft rock" layer represents layers 2 and 3, and "Rock" is layer 1. The faint vertical line immediately right of the "soft soil" label shows the location of the site chosen for 1D ground motion simulations, and the position of the profile is shown in Figure 3.***

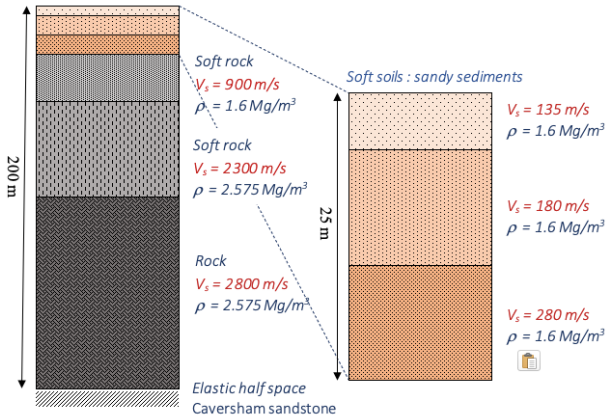


***Figure 5: The St Beach profile soil column developed for OpenSees site effects analysis. The shear wave velocity and mass density of each layer is specified on the right of the main column and inset.***

***Table 1: OpenSees St Beach profile soil column parameters for the six layers in the column. Layer 1 is the deepest layer (rock), as shown in Figure 4, and layer 6 is the shallowest (soft soils). See the explanations of column abbreviations at the base of the table.***

| L | $V_s$ | $\rho$ | Th | Coh | G | E | K |
|---|---|---|---|---|---|---|---|
| 6 | 135 | 1.6 | 5 | 30 | 29160 | 72900 | 48600 |
| 5 | 180 | 2.0 | 10 | 80 | 64800 | 162000 | 108000 |
| 4 | 280 | 2.2 | 10 | 160 | 172480 | 431200 | 287467 |
| 3 | 900 | 2.3 | 25 | n/a | 2106000 | 5265000 | 3510000 |
| 2 | 2300 | 2.58 | 50 | n/a | 13621750 | 34054375 | 22702916 |
| 1 | 2800 | 2.6 | 100 | n/a | 20384000 | 50960000 | 33973333 |

*L = Layer ID; $V_s$ in m/s; $\rho$ in Mg/m$^3$; Th = Max thickness in m; Coh = Cohesion in kPa; G, E and K all in kPa*

### Taieri Basin Profile Model

A profile line is also defined at the Taieri Basin site for development of a 2D basin model (Figure 3). Development of the Taieri Basin profile follows the same overall approach to that of the St Beach profile, but with significant differences in terms of data availability, geology, and basin geometry. Development of the profile is based on [30], and gravity studies [20,22]. Specifically, gravity studies and limited drill-hole data show the Taieri Basin to be deepest on the southeast side because of cumulative displacement on the Titri Fault (Figure 6). Three layers, namely Quaternary, Cretaceous-Tertiary, and schist basement are distinguished in the profile model (Figure 7), and the parameters assumed for the profile layers are listed in Table 2.

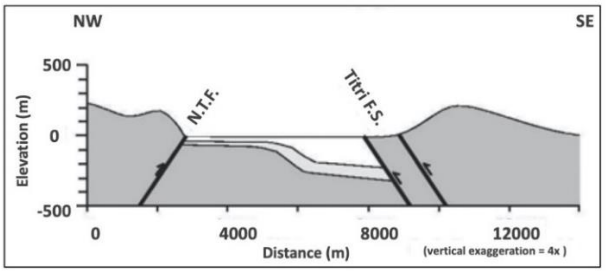


***Figure 6: 2D gravity-based model of the Taieri Basin, showing schist basement in dark grey, Cretaceous-Tertiary sediments in light grey, and Quaternary sediments in white. The Titri and North Taieri faults are also shown [20,22].***

***Table 2: Model parameters that vary between layers in the Taieri Basin profile OpenSees 2D analysis.Layer 1 is the deepest layer (schist basement), as shown in Figure 7, and layer 3 is the shallowest (Quaternary gravels). See the explanations of column abbreviations at the base of the table.***

| L | $V_s$ | $\rho$ | Th | Coh | G | E | K |
|---|---|---|---|---|---|---|---|
| 3 | 200 | 2.07 | 125 | 250 | 82800 | 207000 | 1656000 |
| 2 | 500 | 2.37 | 100 | n/a | 1752852 | 4382130 | 3505704 |
| 1 | 1000 | 2.67 | 250 | n/a | 2670000 | 6675000 | 5340000 |

*L = Layer ID; $V_s$ in m/s; $\rho$ in Mg/m$^3$; Th = Max thickness in m; Coh = Cohesion in kPa; G, E and K all in kPa*

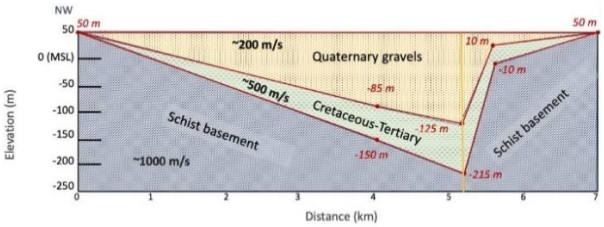


***Figure 7: Taieri basin profile model. The faint vertical line at the position of maximum basin depth marks the location of the site chosen for 1D ground motion simulations, and the position of the profile is shown in Figure 3.***

## SIMULATION METHOD

The overall method of our analysis is portrayed in Figure 8. The process involves: defining sources and sites; ground motion simulations using the SCEC BBP, deconvolution of the time histories to the equivalent bedrock motions; and then 1D and 2D non-linear site response analysis using OpenSees. We describe these steps in more detail in the following sections.

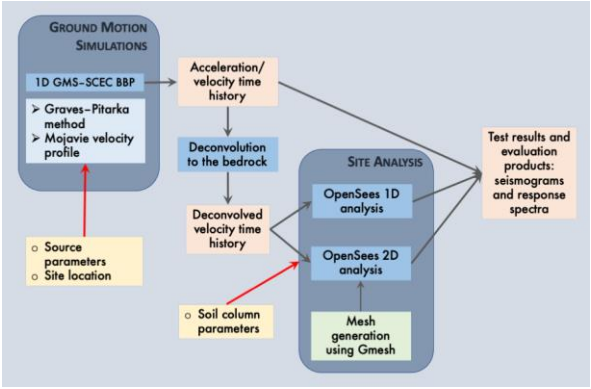


***Figure 8: Schematic of our simulation workflow. Blue rectangles represent applied processes and analyses, yellow represents crucial user-defined input and peach represents test products.***

### Source Parameters

Table 3 summarises the source parameters developed for the Akatore and Hyde faults, including geometrical parameters, and the estimated earthquake magnitude for each source. The geometrical and magnitude parameters for the two faults are taken from [9] , [23] and [34]. The hypocentres on the two faults are simply chosen to represent a unilateral rupture originating at the south end of each fault, and near the base of the seismogenic thickness. A unilateral rupture from south to north on the Akatore Fault would produce strong shaking for Dunedin due to directivity effects (e.g. [35]). These effects would not be present for the Hyde Fault, as the northwards propagating rupture scenario would rupture away from Dunedin and Mosgiel.

### Simulation Platform

The physics-based ground motion simulations performed in this study for developing time histories at the ground surface at each site use the SCEC BBP. The SCEC BBP synthesises rupture-generated low-frequency deterministic and high-frequency stochastic seismograms. These are produced by wave propagation through shallow 1D velocity layered structures and nonlinear site effect modules, and integrated into a system that readily supports the on-demand computation of broadband seismograms. The regional 1D shear wave velocity profiles available in the SCEC BBP library were limited to North America and Japan, so the profile judged to be most similar to the conditions of eastern Otago was the Mojave profile (soils less than 100 m thick overlying rock).

***Table 3: Source parameters for the Akatore and Hyde fault sources in SCEC BBP input format. Parameter descriptions are given at the base of the table.***

| Index | Parameter | Akatore Fault Source | Hyde Fault Source |
|---|---|---|---|
| 1 | MOMENT MAGNITUDE | 7.4 | 7.4 |
| 2 | FAULT_LENGTH [km] | 60 | 60 |
| 3 | FAULT_WIDTH [km] | 18.3 | 17 |
| 4 | DEPTH_TO_TOP [km] | 0 | 0 |
| 5 | STRIKE [degree] | 45 | 30 |
| 6 | RAKE [degree] | 270 | 270 |
| 7 | DIP [degree] | 45 | 60 |
| 8 | LAT_TOP_CENTER | −46.148 | −45.457 |
| 9 | LON_TOP_CENTER | 170.119 | 170.107 |
| 10 | HYPO_ALONG_STK | 00.00 | 00.00 |
| 11 | HYPO_DOWN_DIP | 10.00 | 10.00 |
| 12 | DWID | 0.5 | 0.5 |
| 13 | DLEN | 0.5 | 0.5 |
| 14 | CORNER_FREQ | 0.15 | 0.15 |

*1=Magnitude of full length rupture of fault; 2=Length of full fault rupture; 3=Downdip width of full fault rupture; 4=Depth below ground surface to top of fault; 5=Fault strike; 6=Slip direction of the hanging wall block; 7=angle of the fault plane from the horizontal; 8=Latitude of the midpoint of the top of the fault in decimal degrees; 9=Longitude of the midpoint of the top of the fault in decimal degrees; 10=Distance of hypocentre along strike from southernmost point of the fault; 11=Downdip distance to hypocentre from top of fault; 12=Downdip discretisation distance for fault model; 13=Along-strike discretisation distance for fault model; 14=Corner frequency assumed for fault model.*

The simulation method used in this study is the Graves–Pitarka method [36,37], which is the method of choice for other ground-motion simulation studies in New Zealand [5,38]. The method is hybrid, as it computes the low frequency and high frequency ranges separately prior to being combined into a single time history. The overall computations are deterministic at frequencies below 1 Hz, and stochastic at frequencies above 1 Hz. The use of these different simulation approaches is a consequence of seismological observations, in that source radiation and wave propagation effects tend to become stochastic at frequencies above about 1 Hz. This is a reflection of our relative lack of knowledge at these higher frequencies [36,37]. The Akatore and Hyde fault models are parameterised according to Table 3 for use in the SCEC-BBP and Graves-Pitarka method.

### Deconvolution

In this study 1D and 2D site response analyses are undertaken to better represent the influence of soil and basin characteristics on site amplification. In order to make use of the outputs of the physics-based ground motion simulation, the outputs of this analysis need to be deconvolved from the ground surface to bedrock. Because all of the possible site profiles in the SCEC BBP have some soil above rock, the effects of the soil must be

removed (deconvolved) from the simulations before progressing to nonlinear site response modelling. The process involves inverting the 1D simulations to obtain the equivalent bedrock simulations at depth. The deconvolved bedrock motions are then run through the 2D profiles using OpenSees to produce the final simulations. A deterministic (in contrast to statistical) deconvolution approach has been implemented, and we refer to this as model base wavelet processing.

The velocity series was deconvolved from ground-motion simulations in the frequency domain using a transfer function for damped soil over an elastic half-space. Ground motions are deconvolved to a depth at which the behaviour of nonlinear sediments is practically negligible [5]. For this operation, it is recommended that input ground motions do not include nonlinear site responses because the deconvolution operation is linear (either linear elastic or an equivalent linear scheme). In our study this recommendation is addressed by deactivating the site response module in the SCEC BBP. The Thomson–Haskell transfer matrix method is then used to derive the rock motions. The Thomson Haskell method is a frequency-domain layer-by-layer method used for body wave propagation and surface wave dispersion problems in a multilayered half-space [10,39]. This method uses the frequency-domain transfer function to deconvolve the input simulation velocities for the shallow layers in the SCEC BBP. Fourier and inverse Fourier transforms convert data to the frequency domain and back to the time domain.

**OpenSees Analyses**

*Introduction*

Site response analyses were performed using the OpenSees object-oriented software framework for simulation applications in earthquake engineering using finite element methods [40]. OpenSees has been developed as the computation platform for research in performance-based earthquake engineering at the Pacific Earthquake Engineering Research Centre. Site response analysis is performed using total stress analysis of a layered soil column workflow [41]. A single soil column is modelled in two dimensions and is subjected to ground motions in a way which accounts for the finite rigidity of the elastic half-space bedrock base. Groundwater is not considered, and the soil is modelled in two-dimensions with two degrees-of-freedom, using the plane strain formulation of the quad element. The force history is obtained as a product of the designated velocity time history, and a constant factor. This factor is defined by multiplying the area of the soil column base, the mass density, and the shear wave velocity of the bedrock [42,43].

*Analysis Parameters*

The analysis is run as a transient object (with a constant time step) using the Krylov–Newton algorithm [44]. The Newton method is the most widely used method for solving nonlinear algebraic equations. Classical Rayleigh damping is assigned to all the elements and nodes for analysis stability, and the damping coefficients and ratio are set according to the OpenSees manual [40]. The former is specified based on lower and higher frequencies, (2*Π*1 and 2*Π*15, respectively, with Π = 3.141592654), and the latter is set as 0.1. The analysis also requires a series of material properties to define the constitutive behaviour of the soil and the underlying half-space. Soil properties include mass density, shear wave velocity, Poisson's ratio, and the elastic modulus [45].

For multilayer models, each layer generally has material parameters separately assigned. The soil profiles (layers with properties assigned to them) for the two profiles are developed based on previous studies (Figures 4-7), and for computational simplicity we assume the material types behave according to Pressure Independent Multi Yield (PIMY).

*Profile Meshes*

The density of the profile meshes are defined to ensure that a sufficient number of mesh elements fit within the wavelength of the shear waves. This ensures that the mesh will capture the main aspects of the propagating waves in the analysis. To ensure this condition is met, we need to define the maximum frequency needing to be resolved, and the number of elements needed to fit within one wavelength of a shear wave at that particular frequency. The horizontal dimension of the elements is set to the minimum vertical soil element size, and the numbers of nodes and elements are computed automatically. The mesh is fixed at the base of the model according to the assumption that the soil is underlain by rock. The finite rigidity of the underlying half-space is addressed using a Lysmer–Kuhlemeyer dashpot [43,46,47].

For the development of the 2D profile meshes, all profile layers (Figures 4-7; Tables 1 and 2) are treated as separate physical groups. The meshes are developed by first defining points along the ground surface every 250 m, and the same was done for the base of the section and boundaries of each layer. The two meshes are shown in Figures 9 and 10.

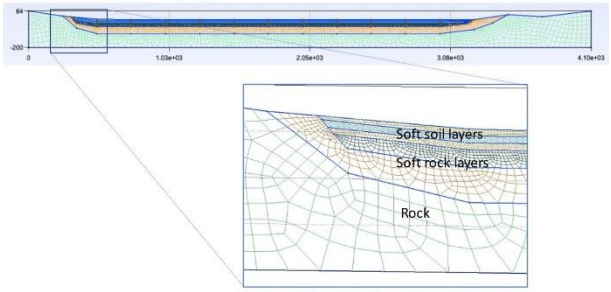


***Figure 9: Mesh for the St Beach profile. Vertical scale = horizontal scale, in metres.***

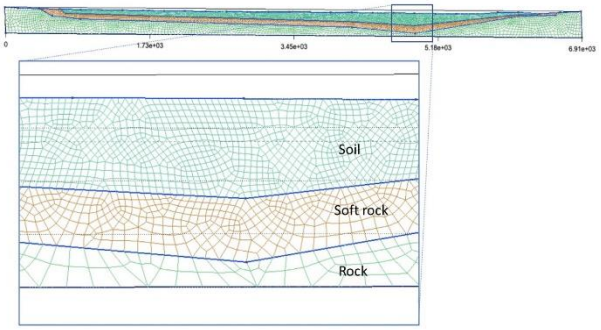


***Figure 10: Mesh for the Taieri Basin profile. Vertical scale = horizontal scale, in metres.***

*2D Analysis*

A 2D site response analysis captures the effect of the sedimentary basins at the two sites, and uses the mesh geometries defined for the associated profiles. Mesh generation is performed with the Gmsh software, using geometry and mesh modules. The geometry module specifies mesh dimensions, layer definitions and mesh resolutions (denser for the shallow layers). The mesh module then applies a 2D Blossom Full-Quad recombination algorithm to generate quadratic elements. Elementary geometrical entities corresponding to each layer are combined into physical groups and exported in formats required by OpenSees.

## RESULTS

### Akatore Fault Earthquake Simulations

*St Beach Site*

Accelerograms are simulated for the horizontal component oriented subparallel to the profile line (E-W for St Beach). The simulations for the Akatore Fault (Figure 11) show a peak ground acceleration (PGA) of 182.7 cm/s$^2$ (0.19 g) at a time of 15.6 s (0.06 Hz). Figures 11b and c show the results for the Akatore Fault scenario, E-W component. The results collectively show significant amplification relative to rock motions.

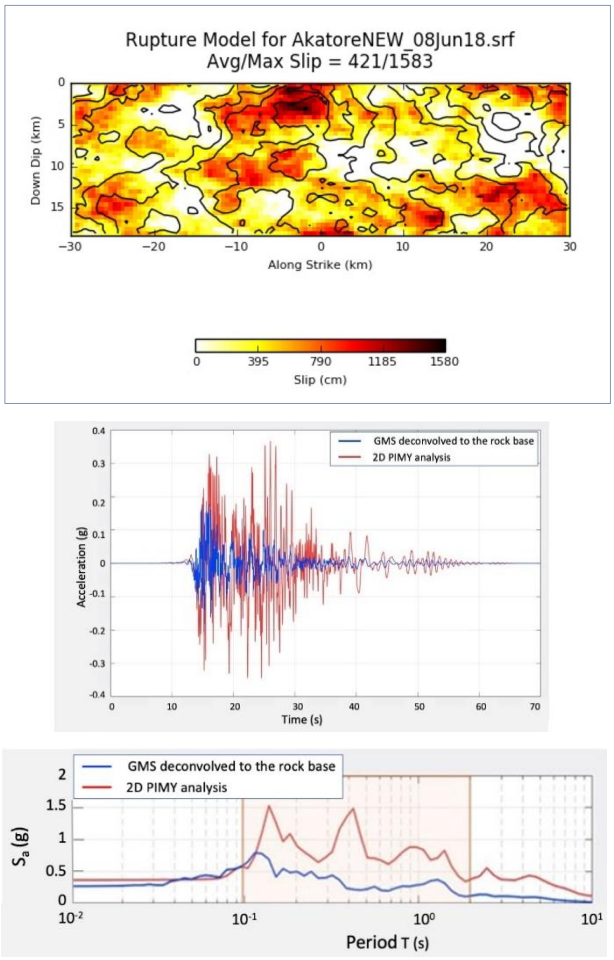


***Figure 11: Fault slip model (top), accelerogram (middle), and pseudo-acceleration response spectra (bottom) for the Akatore Fault−St Beach site earthquake scenario, E−W component (Mw 7.4, distance 15 km).Ground-motion simulations deconvolved to the rock base are in blue, and simulations with 2D site effects analysis included are in red. The shaded area in the bottom plot highlights the period range of most interest to engineering seismic design.***

*Taieri Basin Site*

The simulated seismograms for an Akatore Fault earthquake at the Taieri Basin profile site are shown in Figure 12. The simulations are for the horizontal component oriented subparallel to the profile line (N-S for Taieri profile). The PGA is 283 cm/s$^2$ (0.3 g) for the N-S component, The total duration of shaking for both horizontal components is approximately 45 s. Three-fold amplification can be observed in the seismograms (Figure 12). The amplification appears to be much greater than for the St Beach profile.

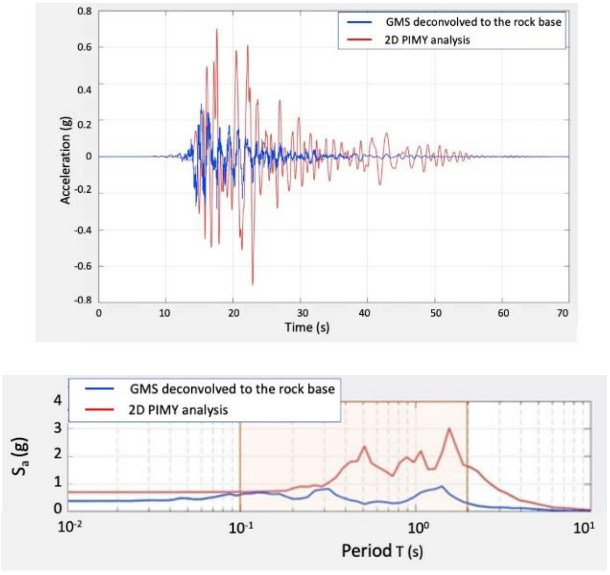


***Figure 12: Accelerogram (top), and pseudo-acceleration response spectra (bottom) for the Akatore Fault−Taieri Basin site earthquake scenario, N−S component (Mw 7.4, distance 15 km). Ground-motion simulations deconvolved to the rock base (in blue), and the 2D site effects analysis (in red). The shaded area is the period range of most relevance to engineering applications.***

### *Hyde Fault Earthquake Simulations*

*St Beach Site*

The simulation results for the Hyde Fault at the St Beach profile are shown in Figure 13. The simulations are for the horizontal component oriented subparallel to the profile line (N-S). The amplitudes are notably smaller than those of the Akatore Fault simulations due to the longer source-to-site distance (50 km vs 15 km). Significant amplification is observed, with a PGA of 0.05−0.1 g at the rock base versus 0.2−0.3 g at the surface (Figures 13 middle and bottom plots).

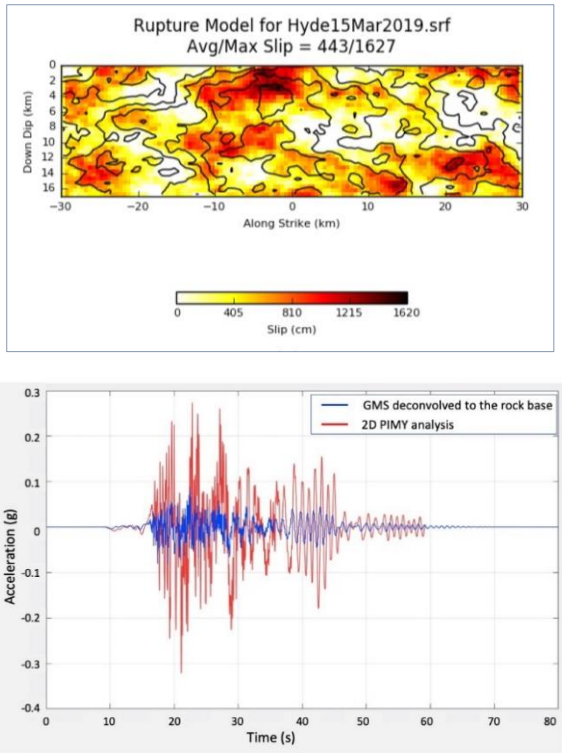

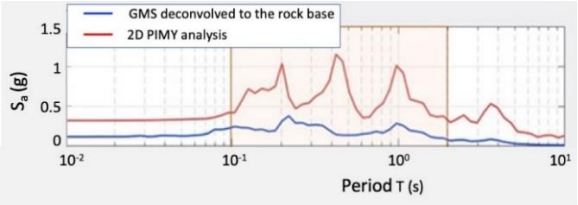


***Figure 13: Fault slip model (top), accelerogram (middle), and pseudo-acceleration response spectra (bottom) for the Hyde Fault−St Beach site earthquake scenario, N−S component (Mw 7.4, distance 50 km).Ground-motion simulations deconvolved to the rock base (in blue), and the 2D site effects analysis (in red). The shaded area in the bottom plot highlights the period range of most interest to engineering seismic design.***

*Taieri Basin Site*

The simulations and rupture model–slip distribution for the Hyde Fault source and Taieri Basin profile are presented in Figure 14. The simulations are for the horizontal component oriented subparallel to the profile line (N-S for Taieri profile). The PGA is 120 cm/s$^2$ (0.1 g), and the total duration of shaking is approximately 55 seconds (longer than for the Akatore Fault). Amplification of greater than a factor of three is apparent at 0.5 Hz, and the resulting amplitudes exceed 0.3 g.

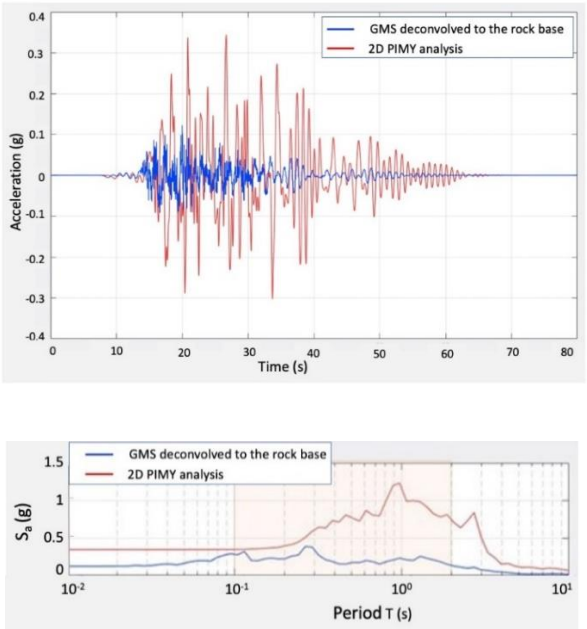


***Figure 14: Accelerogram (top), and pseudo-acceleration response spectra (bottom) for the Hyde Fault−Taieri Basin profile, N−S component (Mw 7.4, distance 40 km).Ground-motion simulations deconvolved to the rock base (in blue), and the 2D site effects analysis (in red). The shaded area in the bottom plot shows the frequency range of most relevance to engineering applications.***

**Ground Motion Simulation Validation**

In order to gain some confidence in our simulations, we perform historical validations on the simulation method by using the one recorded event of significance in Dunedin; the $M_w$ 4.7, 1 June 2015 Lees Valley earthquake. The historical validation method involves comparing simulated spectra for a $M_w$ 4.7 earthquake to recorded spectra for the actual Lees Valley earthquake. The accelerograph stations used in the validation are shown in Figure 15. The validations are limited to the St Beach profile, and to the component orientated subparallel to the profiles (E-W). There are a limited number of stations in Dunedin, and unfortunately none in the Mosgiel area. We select the DKHS and SKFS stations for validation, as they are located approximately 1 km from the St Beach profile and are assumed to have similar soft soil site conditions to those of the site (inferred soil profiles). Table 4 presents the source parameters for the Lees Valley earthquake.

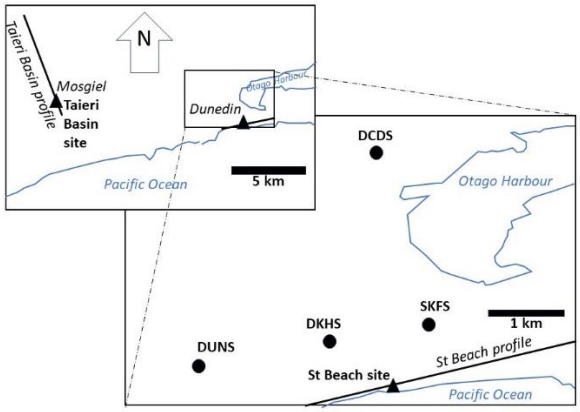


***Figure 15: Location of strong-motion sensors closest to St Beach and Taieri Basin sites/profiles (profiles are shown as black lines, and sites as black triangles). Records from stations DKHS and SKFS are used for validation as they are situated on soft soils and are about 1km from the St Beach site.***

***Table 4: SCEC BBP SRC parameters for the Lees Valley earthquake source.***

| Parameter | Lees Valley Source |
|---|---|
| MAGNITUDE | 4.7 |
| FAULT_LENGTH [km] | 10 |
| FAULT_WIDTH [km] | 10 |
| DEPTH_TO_TOP [km] | 0 |
| STRIKE [deg] | 30 |
| RAKE [deg] | 270 |
| DIP [deg] | 45 |
| LAT_TOP_CENTER | −45.791 |
| LON_TOP_CENTER | 170.135 |
| HYPO_ALONG_STK | 00.00 |
| HYPO_DOWN_DIP | 5.00 |
| DWID | 0.5 |
| DLEN | 0.5 |
| CORNER_FREQ | 0.15 |
| SEED | 3092096 |

**Validation using DKHS and SKFS stations**

The figures below (Figures 16 and 17) compare the simulated and recorded accelerograms and acceleration response spectra for the horizontal component aligned subparallel to the St Beach profile, for the DKHS and SKFS stations. The simulated and recorded data for the two stations appear to show similar overall characteristics in the time histories, but especially so in

the response spectra. The only major departure between observations and simulations are at about 0.1 second period, where the simulations show higher accelerations than the observations for the DKHS and SKFS stations.

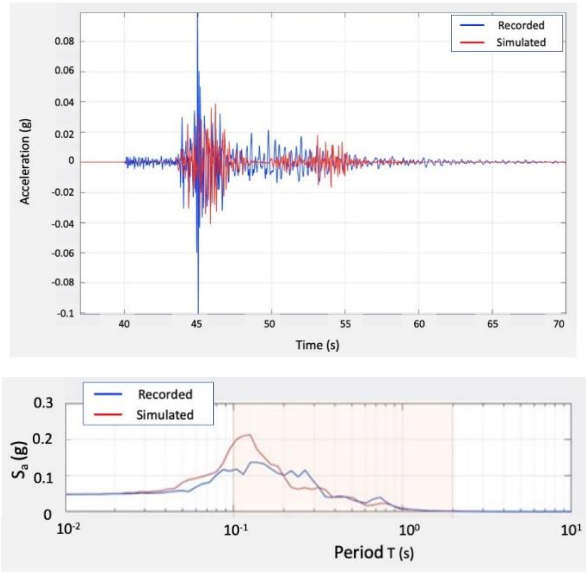


***Figure 16: Recorded (blue) versus simulated (red) horizontal E-W component for the DKHS station, for the 2015 Lees Valley earthquake (Mw 4.7, distance 30 km): (top) seismograms; and (bottom) pseudo-acceleration response spectra. The shaded area indicates the period range of most relevance to engineering applications.***

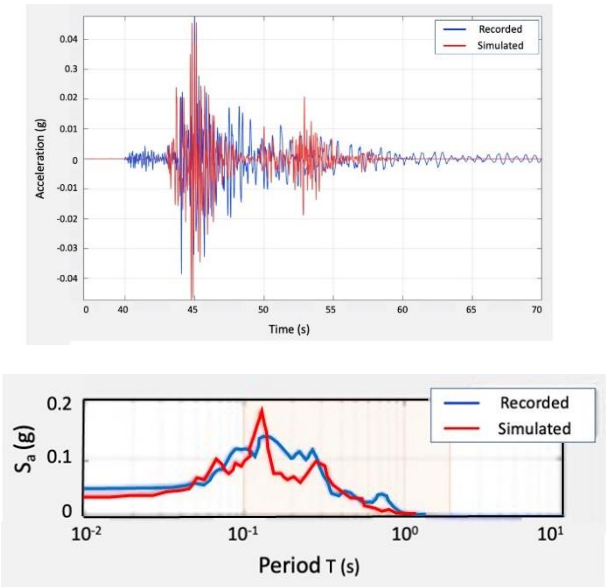


***Figure 17: Recorded (blue) versus simulated (red) horizontal E-W component for the SKFS station, for the 2015 Lees Valley earthquake (Mw 4.7, distance 30 km): (top) seismograms; and (bottom) pseudo-acceleration response spectra. The shaded area indicates the period range of most relevance to engineering applications.***

It is worth noting that the validations have considerable limitations in terms of being focused on small magnitude earthquakes, in contrast to the large magnitude earthquakes represented by the Akatore and Hyde fault simulations. These limitations are unavoidable given the total absence of large-magnitude earthquakes recorded at local distances in the Otago region. Another method of validation would be to compare the spectra for the simulated earthquakes to the outputs of empirical ground motion models. This was outside of the scope of the thesis on which this paper is based, but could form the basis for follow-up work.

(a)

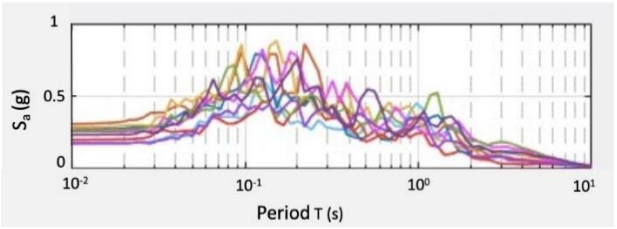


(b)

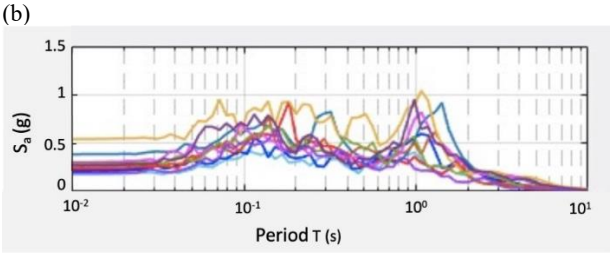


(c)

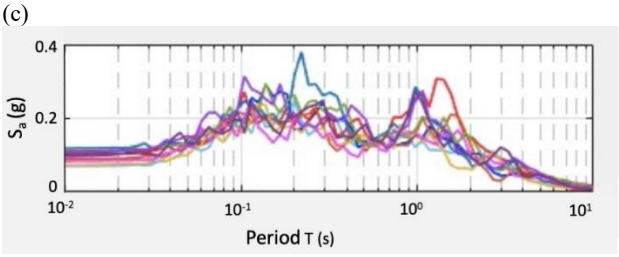


(d)

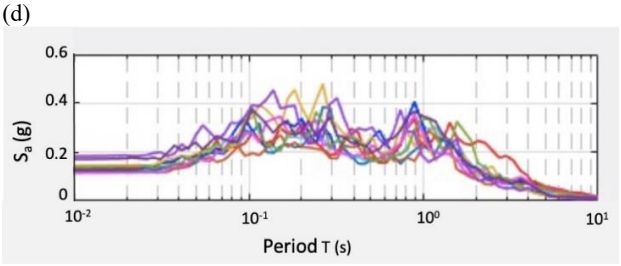


***Figure 18: Akatore and Hyde fault simulations, showing 10 realisations of acceleration response spectra for: (a) Akatore Fault-St Beach, E–W component (Mw 7.4, distance 15 km); (b) Akatore Fault–Taieri Basin site, N–S component (Mw 7.4, distance 15 km); (c) Hyde Fault–St Beach, N–S component (Mw 7.4, distance 50 km),; and (d) Hyde Fault–Taieri Basin, N-S component (Mw 7.4, distance 40 km).***

## SIMULATION UNCERTAINTIES

The development of multiple simulations at a site from a scenario earthquake source is a prudent way to quantify uncertainty and assess methodological stability [48]. To quantify uncertainty in the simulated motions at each source–site combination resulting from fault slip variability, we run 10 different realisations of fault plane slip for each of our earthquake sources. Our treatment of uncertainty is limited to the source and does not include site or basin response uncertainty as part of this study. The resulting acceleration response spectra are shown in Figure 18. The ranges of spectral amplitudes across the 10 simulations are as much as 0.5 g at the 0.1-0.3 second period, and less than half that value elsewhere for the Akatore-St Beach simulations (Figure 18a). Ranges of as much as 0.5g are observed across the 0.07-2 second period for the Akatore-Taieri Basin simulations (Figure 18b). In

contrast, ranges are about 0.1g across the 0.1-2 second period for the Hyde-St Beach simulations (with largest discrepancies at about 0.2-0.3 and 1-2 second periods; Figure 18c). Lastly, the ranges are about 0.1-0.2g at about 0.1-1 second period for the Hyde-Taieri Basin simulations (Figure 18d). Note that we have not formally calculated standard deviations for the differences in the spectra, as these would typically be reported in natural log units of ground motion. The differences above instead serve as an indication of the visual spread of spectra in the graphs.

## COMPARISON TO UNIFORM HAZARD SPECTRA

The development of ground motion simulations in this study represents a "first" for Dunedin and Mosgiel. The simulations provide insight into major earthquakes that have not been observed in the city's 180-year history, and it is informative to compare them to existing hazard estimates. Specifically, we compare the Akatore Fault – St Beach spectra from our simulations (mean, minimum and maximum spectra from Figure 18) to the New Zealand Loadings Standard (i.e. NZS1170.5) 475-year spectra for Class C (Shallow or stiff soil) and D (Deep or flexible soil) sites [49] (see Figure 19). We see that the mean spectrum from the simulations exceeds the NZS1170.5 spectra at the 0.1-0.3 second periods, and also at periods greater than 1 second. Not surprisingly, the maximum-bound simulated spectrum exceeds the NZS1170.5 spectra at all periods. Practically this means that Akatore Fault earthquakes have the potential to produce accelerations in excess of those defined in NZS1170.5 for the range of soils present at the St Beach site. In contrast, our mean simulated spectra are similar to the mean spectra from the 2022 national seismic hazard model (NZ NSHM 2022) [17] for periods less than about 0.2 seconds, but exceed the NZ NSHM 2022 mean spectra at longer periods (Figure 19). We acknowledge the limitations in these comparisons, given that we are comparing deterministic spectra to probabilistic spectra. The comparisons are made in order to show where the simulations stand relative to present loadings standards and latest NSHM spectra.

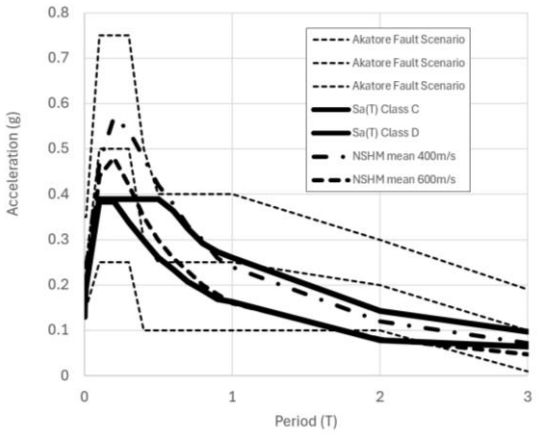


***Figure 19: Smoothed mean, minimum and maximum-bound spectra from our Akatore Fault – St Beach simulations compared to Dunedin NZS1170.5 spectra (Class C and D), and NZ NSHM 2022 spectra (Vs30 400 and 600 m/s), for the 475-year return period. The Vs30 and Class C and D equivalences are based on* [50].**

## CONCLUSIONS

Ground motion simulations for large local scenario earthquakes on the Akatore and Hyde faults have been developed for South Dunedin and Mosgiel using 2D basin and site response modelling. The faults are within 15 and 50 km of the two centres, respectively, and have records of late Quaternary activity (late Holocene in the case of the Akatore). They have however remained quiescent throughout the 180-year history of Dunedin. The simulations have utilised numerical methods and models that explicitly incorporate the physics of the earthquake source and propagation of seismic waves in the areas of interest. A major part of the study has been dedicated to modelling site effects.

The ground-motion simulations have been conducted for two profile lines: the St Beach profile, which runs east–west across South Dunedin, and the Taieri Basin profile, which runs northwest–southeast through Mosgiel township. Some confidence in the simulation results has been gained from the results of a historical validation exercise. The validation has compared simulations of the only instrumentally recorded earthquake of significance in the region (the $M_w$ 4.7 2015 Lees Valley earthquake) to the recorded motions from that event. The simulations and recordings show general compatibility in amplitude and duration.

The uncertainty in the simulated ground motions due to source have also been quantified, and the spectra have also been compared to pre-existing spectra for Dunedin. The range of simulated spectral amplitudes computed for each source-site scenario (10 simulations per scenario) is approximately 0.5 g. The Akatore – St Beach spectra have also been compared to NZS1170.5 and NZ NSHM 2022 spectra, for site classes relevant to those of the St Beach site. In general we see that the simulated spectra exceed the NZS1170.5 spectra at the 0.1-0.3 second periods, but are similar to the mean NZ NSHM 2022 spectra at these periods. Future updates to NZS1170.5 based on NZ NSHM 2022 may therefore be expected to produce design spectra that are more consistent with the results of our study.

Our simulated seismograms are the first ever produced for Dunedin and Mosgiel. As such they constitute a useful source of information for developing realistic earthquake scenarios for the two centres. The simulations demonstrate that strong ground motions will accompany large earthquakes on local sources. This is due to the proximity of the sources, and the presence of soft sediments and basins in the area.

Limitations of the study include: (1) the simulation model being restricted to a 2D analysis rather than full 3D analysis; (2) the validation being restricted to a comparison of spectra from actual versus simulated small-magnitude earthquakes; and (3) the technical incorrectness of comparing scenario (deterministic) spectra to uniform hazard spectra (probabilistic).

## ACKNOWLEDGEMENTS

This project was (partially) supported by Te Hiranga Rū QuakeCoRE, an Aotearoa New Zealand Tertiary Education Commission-funded Centre. Support was in the form of a QuakeCoRE PhD Scholarship for the lead author (Award A914658). This is QuakeCoRE publication number 1014. A writing bursary award from the University of Otago was also greatly appreciated. Hamish Bowman assisted with software and hardware needs, and Fabio Silva assisted with implementing the SCEC BBP. Brendon Bradley, Chris de la Torre, John Ebel, Jennifer Eccles, Robin Lee and Jack Williams are thanked for helpful advice during the course of Anna's PhD. Finally, Liam Wotherspoon is thanked for his co-supervision of Anna's PhD, and for his advice on an earlier version of this manuscript.

## REFERENCES

1 Bommer JJ, Scott SG and Sarma SK (2000). "Hazard-consistent earthquake scenarios". *Soil Dynamics and Earthquake Engineering.* **19**(4): 219-231. https://doi.org/10.1016/S0267-7261(00)00012-9

2 Stirling MW, Pettinga J, Berryman KR and Yetton M (2001). "Probabilistic seismic hazard assessment of the Canterbury region". *Bulletin of the New Zealand Society of Earthquake Engineering*, **34**(4): 318-334. https://hdl.handle.net/10092/17651

3 Lekshmy PR and Raghukanth STG (2019). "Stochastic earthquake source model for ground motion simulation". *Earthquake Engineering and Engineering Vibration,* **18**: 1-34. https://doi.org/10.1007/s11803-019-0487-8

4 Chen S, Xiaolun, L, Fu L and Chen S (2022). "Determination and application of path duration of seismic ground motions based on the K-NET data in Sagami Bay, Japan". *Earthquake Science,* **35**: 4263-279.

5 De la Torre CA, Bradley BA and Lee RL (2020). "Modeling nonlinear site effects in physics-based ground motion simulations of the 2010?2011 Canterbury earthquake sequence". *Earthquake Spectra,* **36**(2). https://doi.org/10.1177/8755293019891729

6 Bradley BA, Bae SE, Polak V, Lee RL, Thomson EM and Tarbali K (2017). "Ground motion simulations of great earthquakes on the Alpine Fault: effect of hypocentre location and comparison with empirical modelling". *New Zealand Journal of Geology and Geophysics*, **60**(3): 188-198. https://doi.org/10.1080/00288306.2017.1297313

7 Holden C, Zhao J and Stirling MW (2013). "Ground motion modelling of a large subduction interface earthquake in Wellington, New Zealand". *Proceedings of the 2013 NZSEE Conference*.

8 Holden C, Kaneko Y, D'Anastasio E, Benites R, Fry B and Hamling IJ (2017). "The 2016 Kaikoura earthquake revealed by kinematic source inversion and seismic wavefield simulations: Slow rupture propagation on a geometrically complex crustal fault network". *Geophysical Research Letters,* **44**(22): 11320-11328. https://doi.org/10.1002/2017gl075301

9 Taylor-Silva BI, Stirling MW, Litchfield NJ, Griffin J, van den Berg EJ and Wang N (2020). "Paleoseismology of the Akatore Fault, Otago, New Zealand". *New Zealand Journal of Geology and Geophysics*, **63**(2): 151-167. https://doi.org/10.1080/00288306.2019.1645706

10 Kowal AF (2022). "*Ground Motion Simulations for Dunedin and Mosgiel, Otago, New Zealand*". PhD Dissertation, University of Otago, Dunedin, NZ.

11 Smith WD (1978). "Earthquake risk in New Zealand: Statistical estimates". *New Zealand Journal of Geology and Geophysics*, **21**(3): 313-327. https://doi.org/10.1080/00288306.1978.10424060

12 Matuschka T, Berryman KR, OLeary A and McVerry G (1985). "New Zealand seismic hazard analysis". *Bulletin of the New Zealand Society for Earthquake Engineering* **18**(4): 313-322. https://doi.org/10.5459/bnzsee.18.4.313-322

13 Stirling MW, Wesnousky SG and Berryman KR (1998). "Probabilistic seismic hazard analysis of New Zealand". *New Zealand Journal of Geology and Geophysics*, **41**(4): 355-375. https://doi.org/10.1080/00288306.1998.9514816

14 Stirling MW, McVerry GH and Berryman KR (2002). "A new seismic hazard model for New Zealand". *Bulletin of the Seismological Society of America*, **92**(5): 1878-1903. https://doi.org/10.1785/0120010156

15 Stirling MW et al (2012). "National seismic hazard model for New Zealand: 2010 update". *Bulletin of the Seismological Society of America,* **102**(4): 1514-1542. https://doi.org/10.1785/0120010156

16 Villamor P et al (2018). "*Unknown faults under cities, GNS Science, Lower Hutt*". GNS Science Miscellaneous Series **124**.

17 Gerstenberger MC, Bora S, Bradley BA, DiCaprio C, Van Dissen RJ, Atkinson GM, Chamberlain C, Christophersen A, Clark KJ, Coffey GL, et al (2022). "*New Zealand National Seismic Hazard Model 2022 Revision: Model, Hazard and Process Overview*". GNS Science Report 2022/5. https:/doi.org/10.21420/TB83-7X19

18 Maechling PJ, Silva F, Callaghan S and Jordan TH (2015). "SCEC broadband platform; system architecture and software implementation*". Seismological Research Letters*, **86**(1): 27-38. https://doi.org/10.1785/0220140125

19 Burks LS and Baker JW (2014). "Validation of ground motion simulations through simple proxies for the response of engineered systems". *Bulletin of the Seismological Society of America*, **104**(4): 1930-1946. https:/doi.org/10.1785/0120130276

20 Litchfield NJ (2001). "The Titri fault system: Quaternary-active faults near the leading edge of the Otago reverse fault province". *New Zealand Journal of Geology and Geophysics*, **44**(4): 517-534. https://doi.org/10.1080/00288306.2001.9514953

21 Todd EK, Stirling MW and Fry B (2020). "Characterising microseismicity in a low seismicity region: Applications of short-term broadband seismic arrays in Dunedin, New Zealand". *New Zealand Journal of Geology and Geophysics*. **63**(3): 1-11. https://doi.org/10.1080/288306.2191707238

22 Barrell DJA, Litchfield NJ, Van Dissen RJ, Wang N, Taylor-Silva B, Hornblow S and Stirling MW (2020). "*Investigation of past earthquakes on the Titri Fault, Coastal Otago, New Zealand*". GNS Science Report 2017/35.

23 Litchfield N, Craw D, Koons, PO, Edge B, Perraudin E and Peake B (2002). "Geology and geochemistry of groundwater within the Taieri Basin, east Otago, New Zealand". *New Zealand Journal of Geology and Geophysics*, **45**(4): 481-497. https://doi.org/10.1080/00288306.2002.9514987

24 Griffin JD, Stirling MW, Barrell DJA, van den Berg EJ, Todd EK, Nicolls R and Wang N (2021). "Paleoseismology of the Hyde Fault, Otago, New Zealand". *New Zealand Journal of Geology and Geophysics,* **65**(4): 613-637. https://doi.org/101080/002883620210.1995007

25 Benson WN and Raeside JD (1963). "Tidal colks in Australia and New Zealand". *New Zealand Journal of Geology and Geophysics,* **6**(4): 634-640. https://doi.org/10.1080/00288306.1963.10420071

26 Cournane S (1992). "*Seismic and oceanographical aspects of lower Otago Harbour*". MSc thesis, University of Otago, Dunedin.

26 Rekker J (2012). "*The South Dunedin coastal aquifer and effect of sea level fluctuations*". Otago Regional Council Report, Dunedin.

27 Fletcher JM, Oskin ME, and Teran OJ, (2016). "The role of a keystone fault in triggering the complex El Mayor-Cucapah earthquake rupture". *Nature Geoscience,* **9**(4): 303-307. https://doi.org/10.1038/ngeo2660

28 Carter RM (1988). "Post-breakup stratigraphy of the Kaikoura Synthem (Cretaceous-Cenozoic), continental margin, southeastern New Zealand". *New Zealand Journal of Geology and Geophysics*, **31**(4): 405-429. https://doi.org/10.1080/00288306.1988.10422141

29 Field BD (1989). "Cretaceous and Cenozoic sedimentary basins and geological evolution of the Canterbury Region, South Island, New Zealand". *New Zealand Geological Survey Basin Studies*, 2.

30 Bishop DG and Turnbull IM (1996). "*Geology of the Dunedin area*". Institute of Geological and Nuclear Sciences, 1:250,000 Geological map 21.

31 McKellar IC (1990). "*Geology of the Southwest Dunedin Urban Area, New Zealand*". Geological Survey, Department of Scientific and Industrial Research, Lower Hutt, NZ.

32 Rattenbury MS and Isaac MJ (2012). "The QMAP 1:250 000 Geological Map of New Zealand project". *New Zealand Journal of Geology and Geophysics*, **55**(4): 393-405. https://doi.org/10.1080/00288306.2012.725417

33 Sangster CA (2019). "*Dunedin Rock and Roll: 3D Seismic Wave Velocity Modelling for Seismic Hazard Analysis*". MSc Thesis, University of Otago.

34 Seebeck H, Van Dissen R, Litchfield N, Barnes PM, Nicol A, Langridge R and Lee J (2023). "The New Zealand Community Fault Model version 1.0: An improved geological foundation for seismic hazard modelling". *New Zealand Journal of Geology and Geophysics*, **67**(2): 209-229. https://doi.org/10.1080/00288306.2023.2181362

35 Somerville PG, Smith NF, Graves RW and Abrahamson NA (1997). "Modification of empirical strong ground motion attenuation relations to include the amplitude and duration effects of rupture directivity". *Seismological Research Letters* **68**: 199-222. https://doi.org/10.1785/gssrl.68.1.199

36 Graves RW and Pitarka A (2010). "Broadband ground-motion simulation using a hybrid approach". *Bulletin of the Seismological Society of America*, **100**(5A): 2095-2123. https://doi.org/10.1785/0120100057

37 Graves R and Pitarka A (2015). "Refinements to the Graves and Pitarka (2010) broadband ground-motion simulation method". *Seismological Research Letters*, **86**(1): 75-80. https://doi.org/10.1785/0220140101 .

38 Lee RL, Bradley BA, Stafford PJ, Graves RW and Rodriguez-Marek A (2020). "Hybrid broadband ground motion simulation validation of small magnitude earthquakes in Canterbury, New Zealand". *Earthquake Spectra*, **36**(2): 673-699. https://doi.org/10.1177/8755293019891718

40 Mazzoni S, McKenna F, Scott M and Fenves G (2009). "*OpenSees Command Language Manual version 2.0*". https://opensees.berkeley.edu/OpenSees/manuals/usermanual/index.html

41 McGann C and Arduino P (2006). "*Site Response Analysis of a Layered Soil Column (Total Stress Analysis)*". OpenSeesWiki: https://opensees.berkeley.edu/wiki/index.php/Site_Response_Analysis_of_a_Layered_Soil_Column_(Total_Stress_Analysis)

42 Joyner WB and Chen ATF (1975). "Calculation of nonlinear ground response in earthquakes". *Bulletin of the Seismological Society of America*, **65**(5): 1315-1336. https://doi.org/10.1785/BSSA0650051315

43 Lysmer J and Kuhlemeyer AM (1969). "Finite dynamic model for infinite media". *Journal of the Engineering Mechanics Division*, **95**: 859-877. https://doi.org/10.1061/JMCEA3.0001144

44 Scott MH and Fenves GL (2010). "Krylov subspace accelerated Newton algorithm: Application to dynamic progressive collapse simulation of frames". *Journal of Structural Engineering*, **136**(5): 473-480. https://doi.org/10.1061/(ASCE)ST.1943-541X.0000143

45 Askeland R (1984). "*The Science and Engineering of Materials*". Brooks/Cole Engineering Division, Monterey, CA.

46 Rajasekaran S (2009). "*Structural Dynamics of Earthquake Engineering: Theory and Application*". Using Mathematica and Matlab, Elsevier Science, Burlington. http://public.ebookcentral.proquest.com/choice/publicfullrecord.aspx?p=1639812

47 Rajasekaran S (2017). "*Structural Dynamics and Earthquake Engineering - CE8021, CE6701 Anna University - Important Questions Answers, Question Paper, Lecture Notes, Study Material*". https://www.brainkart.com/subject/Structural-Dynamics-and-Earthquake Engineering_53

48 Goulet CA, Abrahamson NA, Somerville PG and Wooddell KE (2015). "The SCEC broadband platform validation exercise; methodology for code validation in the context of seismic-hazard analyses". *Seismological Research Letters*, **86**(1): 17-26. https://doi.org/10.1785/0220140104

49 Standards New Zealand (2004). "*Structural design actions, Part 5: Earthquake actions*". Standards Mew Zealand, Wellington, NZ.

50 Perrin ND, Heron D, Kaiser A and Van Houtte C (2015). "VS30 and NZS 1170.5 site class maps of New Zealand". *Proceedings of the NZSEE Conference*.


## DIGITAL APPENDICES

The following digital appendices are available online via the links: https://zenodo.org/uploads/14957586; and 10.5281/zenodo.14957585

A. Electronic Supplementary Document A - Broadband file format guide, SCECpedia
B. Electronic Supplementary Document B - Thomson–Haskell transform function and deconvolution MATLAB scripts
C. Electronic Supplementary Document C - 1D site analysis, OpenSees script example
D. Electronic Supplementary Document D - 2D site analysis, OpenSees script example